

ORIGINAL ARTICLE

Open Access



Functional characterization of a farnesyl diphosphate synthase from *Dendrobium nobile* Lindl

Daoyong Gong^{1,2†}, Bin Wu^{1†}, Hongting Qin¹, Dezhao Fu³, Shunxing Guo¹, Bochu Wang² and Biao Li^{1*} 

Abstract

Dendrobium nobile Lindl. has been used as a traditional Chinese medicine for a long time, in which the most important compound is dendrobine functioning in a variety of pharmacological activities. Farnesyl diphosphate synthase (FPPS) is one of the key enzymes in the biosynthetic pathway of dendrobine. In this work, we found the expression profiles of *DnFPPS* were correlated with the contents of dendrobine under the methyl jasmonate (MeJA) treatments at different time. Then, the cloning and functional identification of a novel *FPPS* from *D. nobile*. The full length of *DnFPPS* is 1231 bp with an open reading frame of 1047 bp encoding 348 amino acids. The sequence similarity analysis demonstrated that *DnFPPS* was in the high homology with *Dendrobium huoshanense* and *Dendrobium catenatum* and contained four conserved domains. Phylogenetic analysis showed that *DnFPPS* was the close to the *DhFPPS*. Then, *DnFPPS* was induced to express in *Escherichia coli*, purified, and identified by SDS-PAGE electrophoresis. Gas chromatography-mass spectrometry analysis indicated that *DnFPPS* could catalyze dimethylallyl pyrophosphate and isopentenyl pyrophosphate to produce farnesyl diphosphate. Taken together, a novel *DnFPPS* was cloned and functionally identified, which supplied a candidate gene for the biosynthetic pathway of dendrobine.

Keywords: *Dendrobium nobile* Lindl., Farnesyl diphosphate synthase, Bioinformatics, Methyl jasmonate, Dendrobine

Introduction

Dendrobium nobile Lindl. (*D. nobile*) is considered to be a well-known traditional Chinese medicine for hundreds of years (Li et al. 2017), and has been widely used in the therapy of diabetes, gastritis, cancer and age-related diseases (Li et al. 2015; Lv et al. 2020; Nie et al. 2020; Song et al. 2012). The major medicinal components in *D. nobile* are dendrobine, polysaccharides, flavonoids and polyphenols (Bhattacharyya et al. 2015; Li et al. 2021; Luo et al. 2010; Lv et al. 2020; Wang et al. 2019). Among them, as a kind of sesquiterpenoid alkaloid, dendrobine is regarded

as the characteristic compound in *D. nobile*, which has important pharmacological activities. For instance, dendrobine could alleviate liver injury and attenuate gestational diabetes mellitus in mice (Ci et al. 2020; Feng et al. 2020). Dendrobine has high medical value, however, the key enzyme genes involved in the biosynthesis of dendrobine have rarely been studied in *D. nobile*.

It is well known that sesquiterpenoids are synthesized via the isoprenoid pathway, which is the most abundant and extensive metabolic pathway in all prokaryotes and eukaryotes. A large number of primary and secondary metabolites are produced through this pathway (Wang et al. 2014). Isoprenoids are a very essential and diverse class of molecules that exists in various life forms and is derived from isopentenyl diphosphate (IPP) and its isomer dimethylallyl diphosphate (DMAPP), IPP and DMAPP is a common precursor of

[†]Daoyong Gong and Bin Wu contributed equally to this work

*Correspondence: libiao@126.com

¹Institute of Medicinal Plant Development, Chinese Academy of Medical Sciences and Peking Union Medical College, Beijing 100193, China
Full list of author information is available at the end of the article

the MVA (mevalonate) (Abate et al. 2017) and the MEP (2-C-methyl-D-erythritol-4-phosphate) pathways (Lee et al. 2020). In the cytoplasm, the well-characterized MVA pathway synthesizes IPP and DMAPP from acetyl-CoA, which consists of six steps, catalyzed by six corresponding enzymes. Another metabolic pathway for IPP and DMAPP synthesis is the MEP pathway from pyruvate and glyceraldehyde-3-phosphate, which is catalyzed by seven enzymes located in the plastids (Abdul Rahman et al. 2019). The initial reaction of the MVA pathway is catalyzed by acetyl-coenzyme A (CoA) C-acetyltransferase (AACT), which is a class II thiolase that condenses two molecules of acetyl-CoA to acetoacetyl-CoA in a reversible reaction (Vögeli et al. 2018). Then, acetoacetyl-CoA is converted to 3-hydroxy-3-methylglutaryl-CoA (HMG-CoA) by HMG synthase (HMGS) (Flynn and Schmidt-Dannert 2018). HMG-CoA is converted to mevalonic acid (MVA) by the enzyme 3-hydroxy-3-methylglutaryl-CoA reductase (HMGR) (Göbel et al. 2019). Subsequently, MVA produces MVA 5-diphosphate in two consecutive reactions catalyzed by MVA kinase (MVK) and phospho-MVA kinase (PMK). The last step of IPP biosynthesis is catalyzed by diphospho-MVA decarboxylase (MPDC), also named MVA-5-diphosphate decarboxylase (PMD). Different isoprenoids share all the early intermediates, up to farnesyl diphosphate through the MVA pathway. The key step of the pathway is the formation of IPP and DMAPP by isopentenyl diphosphate isomerase (IDI). As shown in Additional file 1: Fig. S1, farnesyl diphosphate synthase (FPPS) is a key enzyme in sesquiterpenoids biosynthesis, which catalyzes the consecutive condensations of DMAPP or GPP with IPP to produce FPP (Srivastava et al. 2015; Wang et al. 2014). FPP is located at the first multi-branch point of the various terpenoid biosynthetic pathways such as sesquiterpenes, triterpenes, carotenoids, gibberellins, sterols, dolichols and ubiquinone (Dhar et al. 2013; Wei et al. 2020).

To date, many *FPPS*s have been cloned and characterized in human, some higher plants, yeast and fungi (Kim et al. 2018; Lee et al. 2017a; Rubat et al. 2017; Sharifirad et al. 2016). Studies indicated that the nucleotide sequence length of *FPPS* varies from 1.0 to 2.1 kb. *FPPS* have different isoforms in some organisms and play important functions. For example, in human, only one *FPPS* was encoded containing two isoforms (Romanelli et al. 2009). In *Arabidopsis thaliana*, there are two *fpps* genes containing three isoforms, and knockout of two genes at the same time would lead to the death of plant (Closa et al. 2010; Keim et al. 2012). Moreover, there was a study reported that the mycorrhizal fungus MF23 (*Mycena* sp.) helped to increase the content of dendrobine in *D. nobile*, while the expression of a *FPPS* was

upregulated, indicating the potential role of the *FPPS* in the dendrobine biosynthesis (Li et al. 2017). However, there is no report about the cloning and functional identification of *DnFPPS*. In this study, we further analyzed the expression profiles of *DnFPPS* in different and under methyl jasmonate treatments. In addition, the correlation between the expression profiles of *DnFPPS*, and contents of dendrobine under methyl jasmonate (MeJA) treatments in *D. nobile* were also investigated. Then, *DnFPPS* was cloned by rapid-amplification of cDNA ends (RACE) approach, analyzed the sequence characterization by bioinformatics approach, and detected the enzyme activity by Chromatography-Mass Spectrometer (GC-MS). This study would be helpful for the biosynthesis of dendrobine through engineering in the future work.

Materials and methods

Materials and MeJA treatment

Dendrobium nobile Lindl. seedlings were obtained from Chishui Xintian humintang Pharmaceutical Company Limited (Guizhou, China). Then, seedlings were transplanted into plastic pots (20 cm height and 20 cm diameter) containing a 2:1 mixture of pine bark and sawdust. The plant materials were grown in a glass house at 24–28 °C under natural light and watered twice a week. Subsequently, the biennial plant materials (average height, 25 ± 10 cm, n = 9; number of mature green leaves, 7 ± 3 cm, n = 9) were treated with MeJA (Sigma-Aldrich), and each group consisted of at least five plants. Plant materials were sprayed thoroughly until run-off with 100 µM of MeJA solution prepared in MilliQ water containing 0.5% (v/v) absolute ethanol and covered with polyethylene bags. After 0.5 h of treatment, the polyethylene bags were taken out and then the plant materials were transferred to the glass house. The control plant materials were sprayed with same solution without MeJA, and the other steps were the same as the MeJA spraying group, and isolated from the MeJA-treated plant materials, but the plant materials under the same treatment and growth conditions as the MeJA-treated plant materials. After treatment at the same time, the stems and leaves of the plant materials were harvested, immediately frozen them in liquid nitrogen, and stored at -80 °C ultra-low temperature refrigerator to further separate metabolites and RNA. The leaves were collected at 0 h, 0.5 h, 1 h, 2 h, 4 h, 8 h, 16 h, 24 h, 7 d, 14 d, 21 d and 28 d after incubation for analysis of expression level of *DnFPPS*. The stems were collected at 0 d, 7 d, 14 d, 21 d and 28 d after incubation for determination the content of dendrobine. In addition, *DnFPPS* expression profile was detected by collecting materials from different tissues (roots, stems, leaves and flowers) of the uninduced group.

RNA extraction, detection and reverse transcription

Total RNA of *D. nobile* samples, including different tissue and MeJA-treated were extracted according to the RNeasy Pure Plant Kit (Polysaccharides and Polyphenolics-rich) (TIANGEN, China) manufacturer's instructions. To generate the cDNA representative of MeJA-induced transcription, *D. nobile* plants treated with 100 μ M MeJA were used as the test samples, whereas non-treated plants were used as the control samples. Then, leaf samples from the two groups of plants (the MeJA-treated plants and the non MeJA-treated plants) were collected for RNA extraction. After extraction, total RNA was detected by electrophoresis on a 1.0% agarose gel. Then, the concentration and quality of total RNA were determined the Thermo Scientific NanoDrop 2000/2000c Spectrophotometer. Finally, reverse transcription was performed according to the Thermo Scientific RevertAid First Strand cDNA Synthesis Kit (Thermo Fisher, USA) following the manufacturer's instructions.

Analysis of the expression profiles of *DnFPPS* by quantitative reverse transcription PCR (qRT-PCR)

Firstly, reverse transcription was performed using 500 ng total RNA for each sample and the primers used were presented in the Table S1 (FPPS-1-RT-F/R). The resulting cDNA was diluted 10-fold. qRT-PCR reactions (15 μ L volume) consisted of 7.5 μ L TB Green[®] Premix Ex Taq[™] II (Tli RNaseH Plus), 2 μ L of diluted cDNA, 10 mM of each forward and reverse gene-specific primer, and sterile ddH₂O. Then, qRT-PCR was performed by LightCycler[®] 480 II (Roche) using the conditions: 95 °C for 5 min, 40 cycles of 95 °C for 30 s, 60 °C for 30 s and 72 °C for 15 s.

The GAPDH was used as the endogenous control for qRT-PCR because it is relatively stable in samples of different tissues and MeJA treatment. Subsequently, the melting curves were analyzed at the dissociation step to test the specificity of amplification. Relative gene expression was analyzed following the $2^{-\Delta\Delta C_t}$ method (Kenneth and Thomas 2002).

Extraction and analysis of dendrobine from *D. nobile* under MeJA treatments

The stems collected after incubation for 0 d, 7 d, 14 d, 21 d and 28 d were collected for determination of dendrobine content. After the stems of each treatment were dried at 55 °C, they were thoroughly mixed with a pestle and mortar and ground into a fine powder. The dendrobine standard and internal standard naphthalene used in the experiment were purchased from Sinopharm Chemical Reagent Co., Ltd. and China Food and Drug Control Institute respectively. The GC analysis samples were

prepared in accordance with the Chinese Pharmacopoeia (2020). Chromatography was performed on an Agilent 6890 GC-FID, using an Agilent DB-1 capillary column (0.25 μ m \times 0.25 mm \times 30 m) and nitrogen as the carrier gas.

The experimental sample was repeated at least three times. The samples were analyzed in random order. Each injection of 1 μ L for analysis. The parameters and methods of gas chromatography analysis refer to the Chinese Pharmacopoeia (2020). The flame ionization detection was used to extract the components of the total ion chromatogram. The relative correction factor of naphthalene and dendrobine was obtained ($f=0.002734$). The linear regression equation $y=0.1176x+0.0907$ ($R^2=0.9991$) proved that the concentration of dendrobine was linear, and the peak area is in the range of 4.6–23.0 mg·L⁻¹.

Cloning of a *DnFPPS* from *D. nobile*

The *FPPS* was obtained from our transcriptome data as described previously (Li et al. 2017). Because the sequences did not contain intact ORF, we amplified the 3' and 5' sequences of gene by RACE approach. The RACE primers were subsequently designed using Primer Premier 5.0 (Additional file 1: Table S1). After PCR amplification, the PCR product was purified and cloned into pMD19-T vectors (TAKARA, Japan), and sequenced by Sanger method (GENEWIZ). After aligning and assembly, the full-length cDNA sequences of the *DnFPPS* was deduced. Then, the full-length of *DnFPPS* was amplified by PCR using a pair of specific primers containing restriction sites (Additional file 1: Table S1). Finally, the PCR product was purified and cloned into pMD19-T vectors (TAKARA, Japan), and sequenced by Sanger method (GENEWIZ).

Bioinformatics analysis

The cloned sequences were compared and analyzed via online BLASTn. The nucleotide sequence, deduced amino acid sequence and ORF were analyzed by DNASTAR and ORF Finder, and the sequence comparison was conducted through a database search using BLASTp. *DnFPPS* and other *FPPS*s retrieved from NCBI were aligned using Clustal W. A phylogenetic tree was constructed using maximum likelihood method by MEGA 7 (Additional file 1: Table S2) (Han et al. 2021). The theoretical isoelectric point and molecular weight of the protein were predicted by the ExpASY (Bhattacharya et al. 2018). Multiple sequence alignments were performed using DNAMAN Version 6 (Lynnon Biosoft, San Ramon, CA, USA) (Yang et al. 2020), and spatial structural modeling was accomplished using ExpASY's Swiss-Model and PyMOL software (Yu et al. 2021).

Construction of protein expression vector and transformation into *Escherichia coli* strains

The specific primers containing the restriction sites were designed with Primer Premier 5.0 (Additional file 1: Table S1), and the double restriction sites were introduced by PCR amplification. PCR was performed in 50 mL volume, containing 1× PCR buffer, 0.4 mM of the two primers (FPPS-1-F-BamHI/ FPPS-1-R-xhoI), 0.4 mM dNTP, 2.5 units of LA-Taq DNA polymerase (TAKARA), and 1 mL the *D. nobile* cDNA under the condition: 95 °C for 3 min, 35 cycles of 95 °C for 30 s, 67 °C for 1 min, and 72 °C for 2 min. Then, the PCR products and the expression vector pET-28a were double digested with BamHI/XhoI, and the digested products were used for the ligation reaction after gel recovery to form pET-28a-DnFPPS. Finally, the protein expression vector pET-28a-DnFPPS was transformed into *E. coli* BL21(DE3) competent cells by heat shock approach, and screened by Luria-Bertani (LB) plates with 50 µg/mL kanamycin (Gao et al. 2019) The transformed colonies were confirmed by PCR and sequencing, to confirm the transformation of pET-28a-DnFPPS.

Recombinant FPPS protein induction and purification

The transformed colonies were cultured in 150 mL of LB medium and incubated at 37 °C (150–200 rpm) until the culture reached $OD_{600}=0.8-1.0$. Then 0.5 mM IPTG was added and the induction temperature was set at 16 °C overnight. Then, the bacteria were harvested by centrifugation at 4000×g for 30 min. Subsequently, 0.02 M PBS (phosphate buffer saline) was added, and the cells were broken by an ultrasonic cell disruptor. Finally, the his-tagged protein purification kit (Cwbio, China) was used to purify the crude proteins. SDS-PAGE was used to detect the expression of the recombinant protein (Zha et al. 2016). In brief, SDS-PAGE was performed at a 10% electrophoresis gel and stained with Coomassie brilliant blue. After bleaching, a ChemiDoc™ imaging system (BIO-RAD) was used to observe the results.

Enzyme activity detection and product identification by GC–MS

The DnFPPS activity was determined by transforming IPP and DMAPP to produce FPP. We put 2 mM MgCl₂, 5 mM of DL-Dithiothreitol, 50 µM of DMAPP, 50 µM of IPP, 50 mM of MOPS (pH 7.5) and an appropriate amount of the DnFPPS (0.483 mg/mL) into the reaction mixture with a total volume of 200 µL. The product of the transformed colonies harboring pET-28a was used as a negative control. After incubating overnight at 37 °C, the mixture was extracted with 1-butanol saturated with water, and the diphosphate group was hydrolyzed with potato acid phosphatase at 37 °C. The hydrolyzed

products were extracted with n-hexane, filtered with a 0.22 µm membrane filter, loaded on an Agilent J&W HP-5MS column, eluted with N₂ at 1.2 mL/min, detected by Gas Chromatography (GC) (Models 7890B; Agilent Technologies, Palo Alto, CA, USA). The temperature of the oven was first kept at 80 °C for 1 min, then increased to 220 °C at a rate of 10 °C/min, and finally held at this temperature for 10 min. The injector and transmission line temperatures were set at 200 and 250 °C, respectively. The detection of the analytes was performed using a mass spectrometer (MS) (Models 5977 A; Agilent Technologies) and the Nist11 database was used to analyze the compounds.

Statistical analysis

SPSS 19.0 (Chicago, IL, USA) software was used to analyze the significant differences, and the correlation between gene expression profiles and the contents of dendrobine in samples of different time points at the 5% level using unpaired t-test (two-tailed).

Results

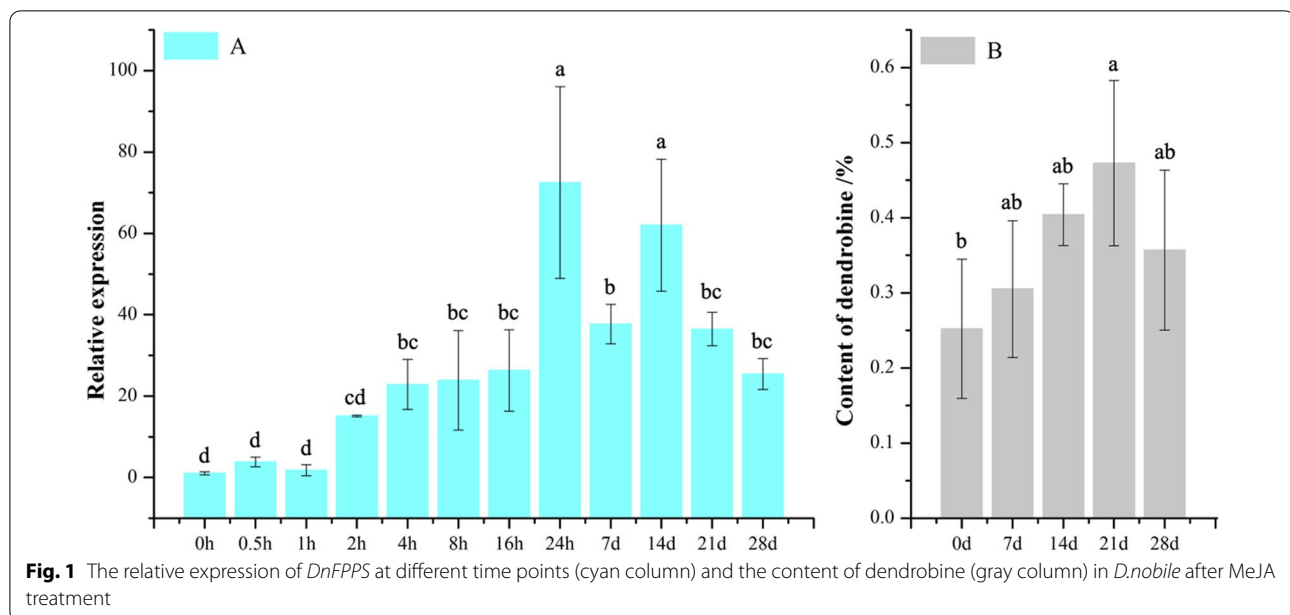
Analysis of expression level of DnFPPS and content of dendrobine under MeJA treatments

qRT-PCR was used to detect the transcription level of *DnFPPS* at different time after MeJA treatment. As shown in Fig. 1 (cyan column), the expression level of *DnFPPS* from 0 to 1 h was relatively low. Then, the expression level of *DnFPPS* was increased after 2 h, and reached the highest at 14 d. The effect of MeJA induction on the content of dendrobine in *D. nobile* is shown in Fig. 1. There was a significant difference in the content of dendrobine in the control group and the experimental group, indicating that MeJA can effectively stimulate the biosynthesis of dendrobine (Fig. 1 (gray column)). Moreover, the expression level of *DnFPPS* was positively correlated with the amount of dendrobine. Therefore, we speculated that *DnFPPS* might participate in dendrobine biosynthesis through MeJA-mediated signal pathway.

The expression profiles of *DnFPPS* in different tissues of *D. nobile* showed the stem > leaf > root > flower (Additional file 1: Fig. S2), consistent with the amount of dendrobine in different tissue (Li et al. 2017), which also implied *DnFPPS* was related to the biosynthesis of dendrobine. Therefore, we further cloned and validated the function of *DnFPPS*.

Cloning of full-length cDNA of DnFPPS

Through our previous transcriptome data, the putative 615 bp fragment of *DnFPPS* was obtained. In order to obtain the full-length sequence of *DnFPPS*, the SMARTer® RACE 5'/3' kit was used to perform PCR amplification according to the instructions. *DnFPPS* was



sequenced after purification. Sequence analysis showed that the length of the cloned DNA was 1231 bp, including the ORF flanked by 80-bp 5'-UTR and 104-bp 3'-UTR. ORF Finder showed that *DnFPPS* contained an ORF with a length of 1047 bp (Electrophoresis results are shown in Additional file 1: Fig. S3) encoding a protein with 348 amino acids. The calculated molecular weight of *DnFPPS* was about 40.31 kDa, and the theoretical isoelectric point was 5.09. The nucleotide sequence of *DnFPPS* has been submitted to the GenBank database under the accession number MZ044976.

Sequence analysis and homology model of the *DnFPPS* protein

On line BLASTp result showed that the deduced *DnFPPS* was in high similarity in amino acid sequence with FPPSs in other plant species, such as DhFPPS from *Dendrobium huoshanense* (98.28%) (accession no. AHC30884.1), DcFPPS from *Dendrobium catenatum* (97.99%) (accession no. XP_020678044.1), DoFPPS from *Dendrobium officinale* (97.41%) (accession no. AFX68799.1), CgFPPS from *Cymbidium goeringii* (91.67%) (accession no. AFP19446.1), PjFPPS from *Phalaenopsis japonica* (90.52%) (accession no. AXQ06578.1), and ArFPPS from *Anoectochilus roxburghii* (87.64%) (accession no. AZP53600.1) (Fig. 2). This suggested that *DnFPPS* belonged to the FPPS superfamily. Sequence alignment of *DnFPPS* with FPPSs derived from other plant showed that there were at least four conserved regions, named I to IV (Fig. 2). The N-terminal extension of the FPPSs of these species were enriched in basic, hydroxylated and hydrophobic residues, and had the RXXS tetrapeptide

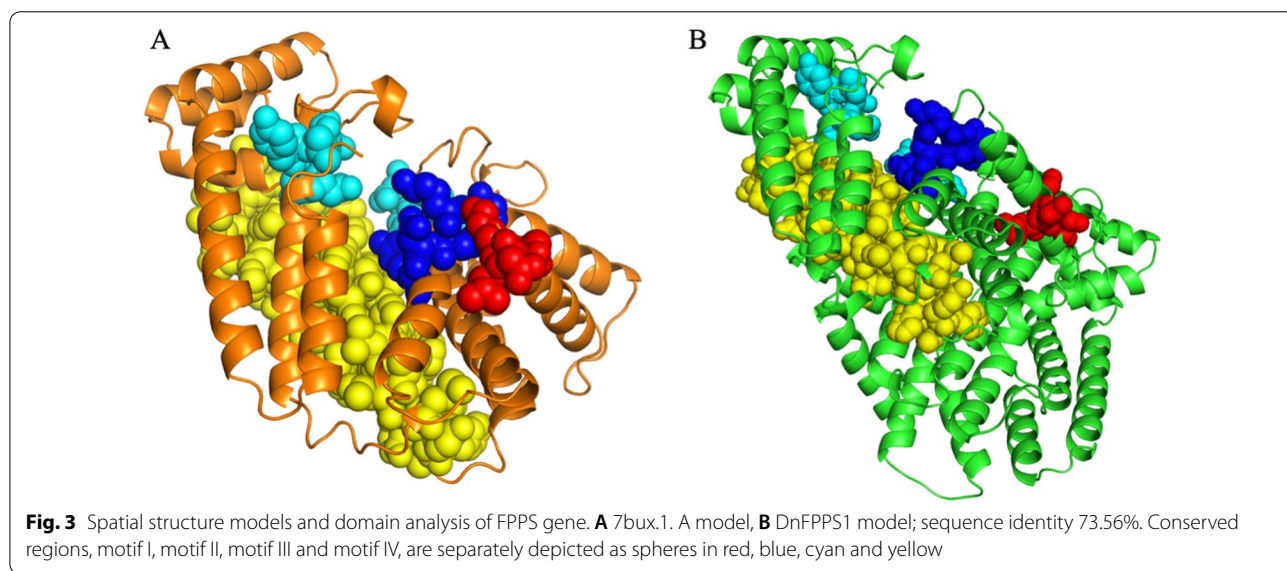
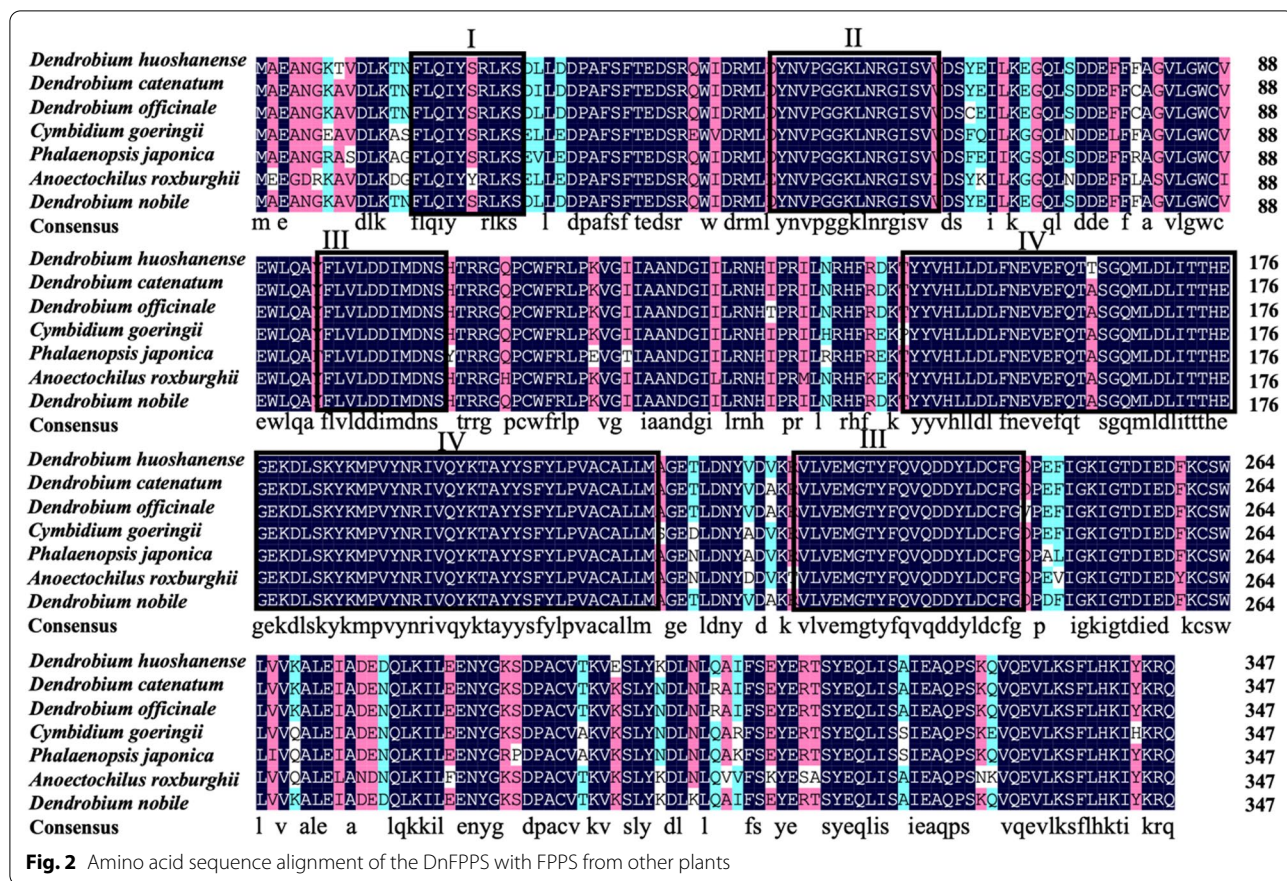
(region I), which was the cleavage motif of mitochondrial targeting peptides. The conserved GGKXXR motif was present in region II. And region II was rich in arginine and lysine, indicating that it may be involved in substrate binding (Blanchard and Karst 1993). The highly conserved aspartate-rich motif (DDXXD) was existed in region III, which were perhaps participated in substrate binding by forming a magnesium salt bridge between the pyrophosphate moiety of the isoprenoid substrate and the carboxyl group of the aspartic acid (Ashby and Edwards 1990) and a very conserved motif (region IV). Subcellular localization predicted that *DnFPPS* was localized in the cytoplasm and plasma membrane with a probability of 87.6%. The tertiary structure prediction of the protein (Fig. 3) was highly similar to that of *Eucomia ulmoides* FPS1(7bux.1. A).

Phylogenetic analysis

The phylogenetic tree was constructed by 14 plant FPPSs obtained from NCBI. Result showed that the 15 plant FPPSs could be grouped into 4 categories, namely *Orchidaceae*, *Asparagaceae*, *Arecaceae* and *Liliaceae* (Fig. 4). The *Dendrobium* FPPSs were clustered into one subgroup, including *DnFPPS*, DhFPPS, DcFPPS and DoFPPS, and the *DnFPPS* was more close to DhFPPS.

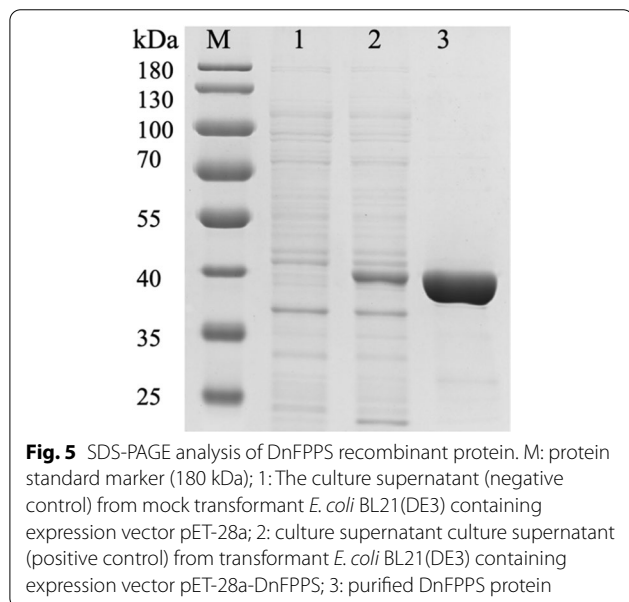
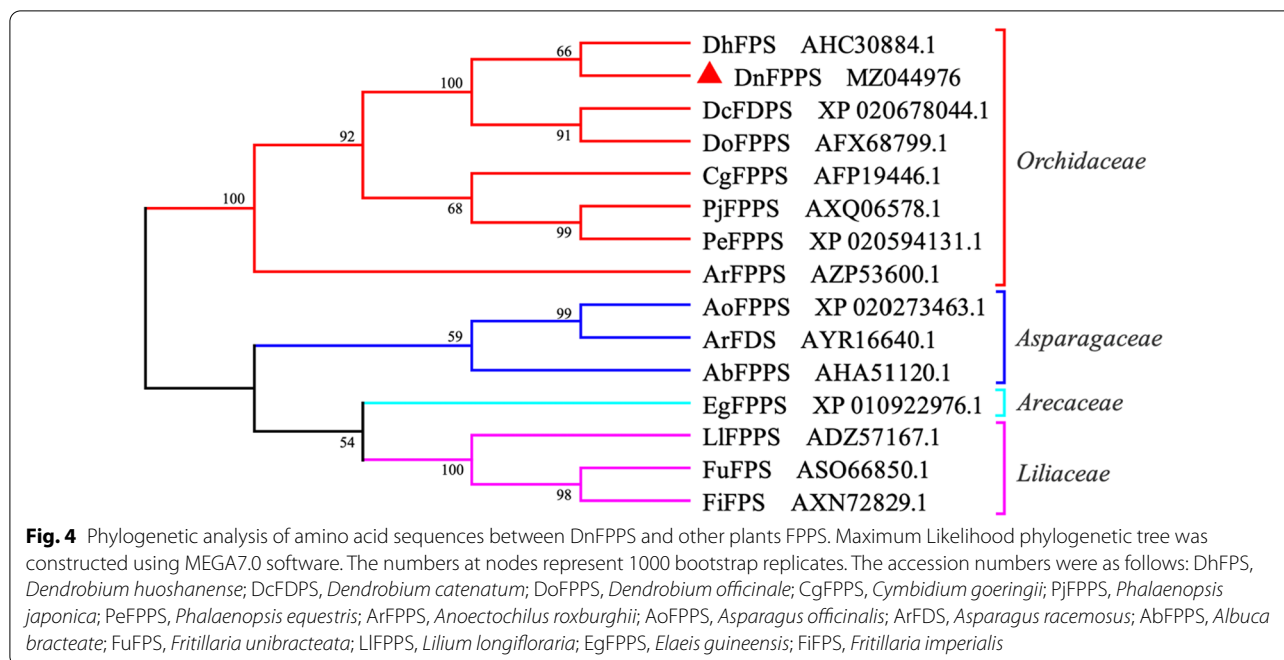
Expression and purification of *DnFPPS* in *E. coli*

In order to screen out clones that can produce the *DnFPPS* protein, 1 positive clone was inoculated into 25 mL shaking flasks containing 25 mL Ampicillin (100 mg/mL), and cultivated at 37 °C, 150 rpm to OD=0.8–1.0. Then, 0.5 mM isopropyl-beta-D-thiogalactopyranoside



(IPTG) was added to the culture and incubated at 16 °C, 150 rpm overnight. Then the cells were disrupted by ultrasonic cell crushing apparatus. Subsequently, sodium dodecyl sulfate-polyacrylamide gel electrophoresis

(SDS-PAGE) was used to detect the expression of the recombinant DnFPPS (Fig. 5). SDS-PAGE was performed on a 10% flowing gel, and the band size was observed after Coomassie brilliant blue staining and decolorization. The



results showed that the molecular weight of DnFPPS was approximately 40 kDa (Fig. 5, line 2), which was consistent with the predicted molecular weight. Finally, the DnFPPS was purified by His-tag by Ni²⁺ chelating chromatography, which showed an obvious single band (Fig. 5, line 3). These above results indicated that the DnFPPS protein were successfully expressed, and purified, and could be used for subsequent enzyme activity detection.

The product of FPPS was determined by gas chromatography–mass spectrometer (GC–MS)

In order to explore the function of DnFPPS, the purified DnFPPS and substrates (IPP and DMAPP) were added to the same reaction system. After the reaction was catalyzed overnight at 30 °C, the mixture was extracted with 1-butanol saturated with water, and then the diphosphate group was hydrolyzed with potato acid phosphatase at 37 °C. Secondly, the hydrolysate was extracted with n-hexane, filtered with a 0.22 μm filter membrane, and the filtrate was analyzed by GC-MS. As shown in Fig. 6, comparing the retention time of the sample with the retention time of FPP-derived farnesane (Fig. 6a), it was confirmed that DnFPPS could catalyze DMAPP and IPP to generate FPP (Fig. 6c). In contrast, no such product peak was detected in the sample extracted from the in vitro reaction mixture containing the mock-transformed *E. coli* mock-purification protocol containing the expression vector pET-28a (Fig. 6e). These results indicated that *DnFPPS* of *D. nobile* is a functional FPPS.

Analysis of the expression profiles of dendrobine biosynthetic pathway genes under MeJA treatments

Seven key enzyme genes, including *AACT*, *HMGs*, *HMGs*, *HMGR*, *MVD*, *PMK* and *MK* in the upstream of FPPS, and a downstream *TPS* potentially involved in the biosynthesis of dendrobine were screened from the transcriptome data (Li et al. 2017), and their expression levels were verified by qRT-PCR (Additional file 1:

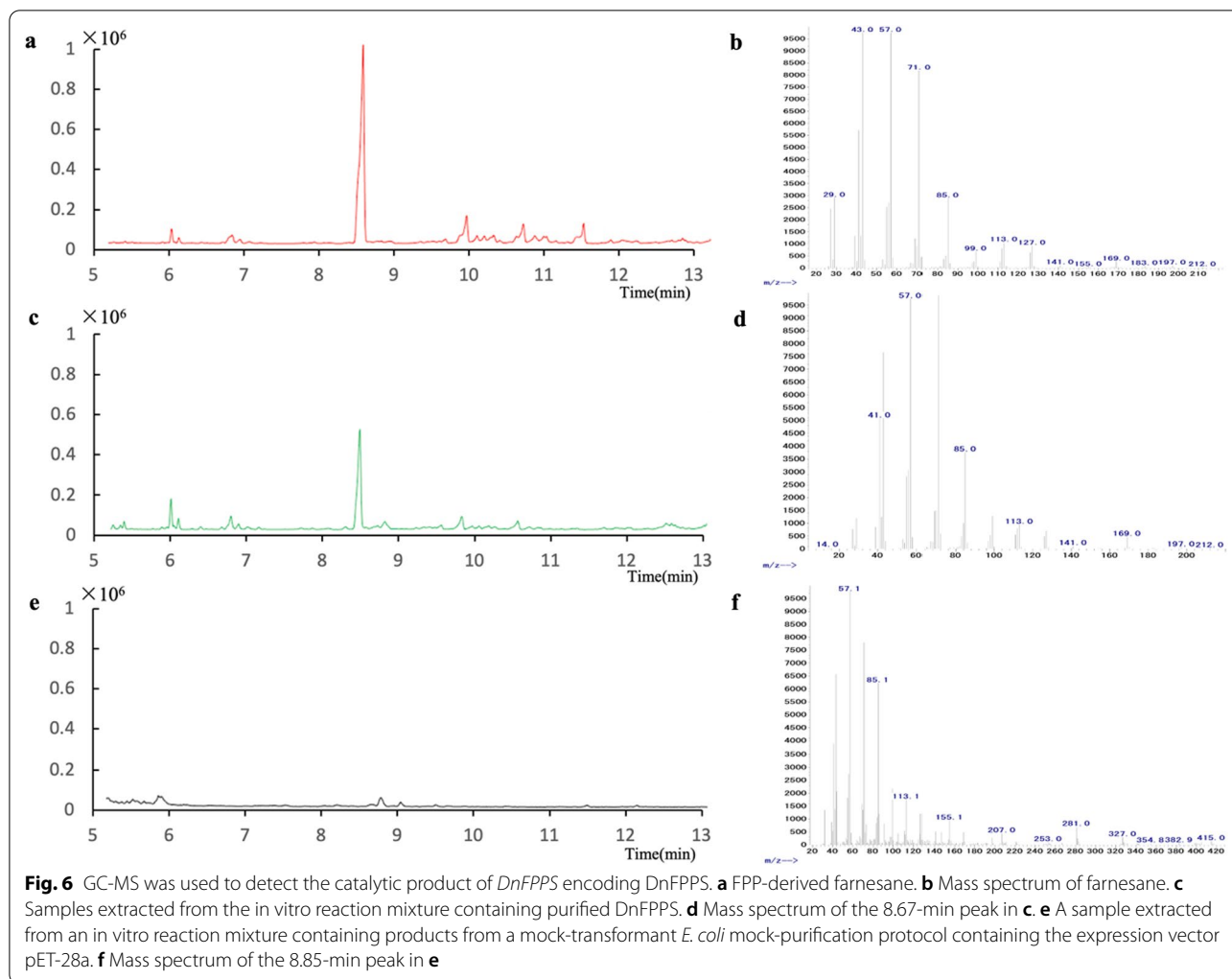


Fig. S4). These Results showed that *AACT*, *HMGS*, *HMGR*, *PMK* and *MK* had no significant correlation with *DnFPPS* (Additional file 1: Table S3) and their relative expression levels were shown in Additional file 1: Fig. S4. While, *MVD* and *TPS21* were significantly correlated with *DnFPPS* gene, and the correlation coefficient was 0.638 and 0.631, respectively.

Discussion

As a class of natural hydrocarbon compounds with isoprene as the structural unit, terpenoids are widely distributed, with diverse in types and rich in structure. FPPS is a key enzyme in the biosynthetic pathway of terpenoids in plants. So far, many scholars have studied the key enzyme genes of *fpps* (Abate et al. 2017; Cao et al. 2012; Cheng and Li 2019; Deng et al. 2016; Dozier and Distefano 2012; Pérez-Castrillón et al. 2014). It is generally believed that FPP is an essential compound for most

linear isoprenoids, sterols, and sesquiterpenes in the biosynthesis (Kajiura et al. 2017). Decades of FPP synthesis studies have identified and characterized many *fpps* genes from bacteria, insects, plants and mammals (Kajiura et al. 2017). In *D. nobile*, FPP is believed to be a key compound in the biosynthetic pathway of dendrobine, and thus there is a meaningful study to elucidate the biosynthetic mechanism of FPP and characterize DnFPPS (Gong et al. 2021). For example, FPP is catalyzed by caryophyllene synthase, germacrene D synthase, squalene synthase and amorpho-4, 11-diene synthase to generate caryophyllene, germacrene D, squalene and amorphadiene, respectively (Gong et al. 2021). Therefore, it is particularly important to explore the sesquiterpenoid skeleton intermediates formed by DnFPPS in the biosynthesis pathway of dendrobine.

Due to dendrobine having sesquiterpene skeleton, its biosynthetic pathway is similar to other sesquiterpene

compounds. Dendrobine was separated from *D. nobile* in early 1932 by H. Suzuki (Suzuki 1932). Later, in 1935, Chen isolated the compound from *D. nobile* (Chen and Chen 1935). However, its sesquiterpene skeleton structure was not initially identified until 1963 by Y. Inubushi (Inubushi et al. 1963). Dendrobine was identified as a tetracyclic system with a five-membered lactone ring structure, containing N-methyl and oxygen in the form of γ -lactone, and its molecular formula is $C_{16}H_{25}NO_2$ (Sando et al. 2008). Subsequently, the tricyclic skeleton structure of dendrobine was synthesized (Kaneko 1970). The complete biosynthetic pathway of dendrobine was reported, the complex steps and low recovery of dendrobine were identified (Corbella et al. 1975; Lee et al. 2017b; Sha et al. 1997; Yamazaki et al. 1966). Dendrobine is still the main source of *dendrobium* plant extraction and the key enzymes genes in the biosynthetic pathway of dendrobine are rarely reported. Therefore, how to reconstruct dendrobine biosynthesis pathway in vitro has become a key problem to be solved urgently.

In this study, we have isolated *DnFPPS* from *D. nobile*, and analyzed the characterization of *DnFPPS* by bioinformatics approach. The full length of *DnFPPS* is 1231 bp with an open reading frame of 1047 bp encoding 348 amino acids. It was predicted that the relative molecular mass of *DnFPPS* protein was 40.31 kDa and the isoelectric point was 5.09. Through homology analysis and phylogenetic tree analysis, we known that the nucleotide sequence similarity of the FPPS between *D. nobile* and *D. huoshanense* (AHC30884.1) was 98.28%. *DnFPPS* was expressed in the recombinant *E. coli* and purified. In order to determine *DnFPPS* as a functional gene encoding FPPS, purified *DnFPPS* was used to catalyze DMAPP and IPP to synthesize FPP. GC-MS test confirmed that the *DnFPPS* gene from *D. nobile* is a functional gene encoding FPPS. The results indicated that the activity of FPPS in *D. nobile* was nonlinearly correlated with the content of dendrobine. As far as we know, this is the first report about gene cloning and characterization from *D. nobile*. Our results will be helpful to facilitate the investigation of its structure, expression and the role of FPPS in the control of dendrobine biosynthesis in *D. nobile*. In addition, we also explored some other genes involved in dendrobine biosynthesis pathway, and found that the terpenoid synthase gene (*TPS21*) was significantly correlated with *DnFPPS* gene and its relative expression level was consistent with that of *DnFPPS* gene. Therefore, we speculated that *TPS21* might be a key enzyme gene involved in dendrobine biosynthesis pathway. However, we cannot exclude other key enzyme genes from participating in the dendrobine biosynthesis pathway, because on the one hand, these genes were a large gene family,

and we only selected one of the genes with significant differences in the transcription set induced by mycorrhizal fungi (MF23) as a reference for relative expression levels. On the other hand, other genes may be the same function after induction of methyl jasmonate, but we haven't found it yet.

To date, we have initially explored the function of FPPS, which is far from enough for the biosynthetic pathway of dendrobine. For example, knockdown of the *MpFPPS1/2* gene significantly reduced the proportion of droplets released by aphids and the (E)- β -farnesene content (Cheng and Li 2019), this result suggest that both *fpps* genes are involved in the production of (E)- β -farnesene in *Myzus persicae*. In addition, more experiments should be conducted in the future to further explore the role and molecular mechanism of FPPS in the biosynthesis of dendrobine. Future research will focus on the use of inhibition, transgene, RNAi and other technologies to verify the function of the *DnFPPS*, in order to intuitively and accurately clarify the molecular mechanism of FPPS. For example, the activity of human FPPS, *EuFPPS*, and *PcFPPS* is inhibited by IPP, suggesting that the active site (which contributes to the binding of allyl substrates) is occupied by IPP close to the first DDxxD motif (Kajiura et al. 2017). Previous studies have shown that two IPP molecules bind to avian FPPS monomers, indicating that IPP can bind to donor and allyl sites (Kajiura et al. 2017; King and Rilling 1977). Thus, there may be potential utilization sites near the active sites of FPPS to control dendrobine biosynthesis. Meanwhile, it has been shown that long N-terminal sequences do not affect the function of *PcFPPS*, because *PcFPPS* contains a RxxS motif, the cleavage site of mitochondrial targeting sequence Arg67-Ser70 (Frick et al. 2013). In general, FPPS enzymes require Mg^{2+} or Mn^{2+} or Co^{2+} as a cofactor for FPP synthesis. Such as Co^{2+} acts as a cofactor in *EuFPPS*, and *PcFPPS* (Kajiura et al. 2017). Therefore, the role of cofactors should also be taken into account when reconstructing dendrobine biosynthesis in vitro.

In short, dendrobine is the main active compound of *D. nobile*, which has a variety of biological activities and considerable economic value. However, its biosynthesis is an extremely complex and dynamic process that is regulated by multiple factors. It is still unclear how the activity of its key enzymes during the growth of *D. nobile* is affected by environmental factors, and the relationship between the synthesis of secondary metabolites and key enzymes is unclear. Studies have shown that mycorrhizal fungi can increase the production of dendrobine. However, its molecular mechanism needs to be further explored (Li et al. 2017). In the future, we can focus on studying whether environmental factors in the habitat of

D. nobile affect the expression of *FPPS*, so as to achieve the goal of increasing the production of dendrobine and provide scientific basis for improving the medicinal quality and economic value of *D. nobile*.

Abbreviations

D. nobile: *Dendrobium nobile* Lindl; *E. coli*: BL21(DE3) *Escherichia coli* BL21(DE3); IPP: Isopentenyl diphosphate; DMAPP: Dimethylallyl diphosphate; FPP: Farnesyl diphosphate; MeJA: Methyl Jasmonate; ORF: Open reading frame; IPTG: Isopropyl-beta-D-thiogalactopyranoside; GC-MS: Gas chromatography-mass spectrometer; SDS-PAGE: Sodium dodecyl sulfate-polyacrylamide gel electrophoresis.

Supplementary Information

The online version contains supplementary material available at <https://doi.org/10.1186/s13568-022-01470-2>.

Additional file 1: Table S1. Primers used in this study. Primer sequences for the restriction sites are shown in bold. **Table S2.** Relevant *FPPS* sequences for phylogenetic analysis. **Table S3.** a. Correlation analysis between *AACT* and *FPPS*. b. Correlation analysis between *HMGR* and *FPPS*. c. Correlation analysis between *HMGS* and *FPPS*. d. Correlation analysis between *MK* and *FPPS*. e. Correlation analysis between *PMK* and *FPPS*. f. Correlation analysis between *MVD* and *FPPS*. g. Correlation analysis between *TPS21* and *FPPS*. **Fig. S1** The *MVA* and *MEP* pathways are the main steps in the synthesis of dendrobine. **Fig. S2.** The relative expression of *DnFPPS* at different tissues in *D. nobile*. **Fig. S3** Agarose gelelectrophoresis of the core fragment amplification products of *DnFpps*. **Fig. S4** The relative expression of different genes at different time points in *D. nobile* after MeJA treatment.

Author contributions

BL, SG, ZF and BW made significant contributions to the design of the experiments and the draft the manuscript. BW provided experimental materials for support. DG performed the RACE, vector construction, tissue-specific expression analysis, operated bioinformatic software and analysis, interpreted the data and drafted the manuscript. HQ carried out an experiment to detect the content of dendrobine. All authors reviewed the manuscript. All authors read and approved the final manuscript.

Funding

The research was financially supported by the National Key R&D Program of China (2018YFC1706200 for L. B), Medical science and Health Technology Innovation Project (2021-1-H2M-032 for L. B), the Special Project for Academic Construction of Peking Union Medical College (Tsinghua 211-201920100902), and the National Science & Technology Fundamental Resources Investigation Program of China (2018FY100700).

Availability of data and materials

The raw data supporting the conclusions of this manuscript will be made available by the authors, without undue reservation, to any qualified researcher.

Declarations

Ethics approval and consent to participate

Not applicable.

Consent for publication

Not applicable.

Competing interests

The authors declare that the research was conducted in the absence of any commercial or financial relationships that could be construed as a potential competing interests.

Author details

¹Institute of Medicinal Plant Development, Chinese Academy of Medical Sciences and Peking Union Medical College, Beijing 100193, China. ²College of Bioengineering of Chongqing University, Chongqing 400045, People's Republic of China. ³Beijing Asia-East Bio-pharmaceutical Co., Ltd, Beijing 102200, People's Republic of China.

Received: 22 November 2021 Accepted: 22 September 2022

Published online: 06 October 2022

References

- Abate M, Laezza C, Pisanti S, Torelli G, Seneca V, Catapano G, Montella F, Ranieri R, Notarnicola M, Gazzerri P, Bifulco M, Ciaglia E (2017) Deregulated expression and activity of farnesyl diphosphate synthase (*FPPS*) in glioblastoma. *Sci Rep* 7(1):14123. <https://doi.org/10.1038/s41598-017-14495-6>
- Abdul Rahman SN, Bakar MFA, Singham GV, Othman AS (2019) Single-nucleotide polymorphism markers within *MVA* and *MEP* pathways among *Hevea brasiliensis* clones through transcriptomic analysis. *Biotech* 9(11):388. <https://doi.org/10.1007/s13205-019-1921-3>
- Ashby MN, Edwards PA (1990) Elucidation of the deficiency in two yeast coenzyme Q mutants. Characterization of the structural gene encoding hexaprenyl pyrophosphate synthetase. *J Biol Chem* 265(22):13157–13164. [https://doi.org/10.1016/S0021-9258\(19\)38280-8](https://doi.org/10.1016/S0021-9258(19)38280-8)
- Bhattacharya M, Hota A, Kar A, Sankar Chini D, Chandra Malick R, Chandra Patra B, Kumar Das B (2018) In silico structural and functional modelling of Antifreeze protein (AFP) sequences of Ocean pout (*Zoarces americanus*, Bloch & Schneider 1801). *J Genet Eng Biotechnol* 16(2):721–730. <https://doi.org/10.1016/j.jgeb.2018.08.004>
- Bhattacharyya P, Kumaria S, Tandon P (2015) Applicability of ISSR and DAMD markers for phyto-molecular characterization and association with some important biochemical traits of *Dendrobium nobile*, an endangered medicinal orchid. *Phytochemistry* 117(306):306–316. <https://doi.org/10.1016/j.phytochem.2015.06.022>
- Blanchard L, Karst F (1993) Characterization of a lysine-to-glutamic acid mutation in a conservative sequence of farnesyl diphosphate synthase from *Saccharomyces cerevisiae*. *Gene* 125(2):185–189. [https://doi.org/10.1016/0378-1119\(93\)90326-x](https://doi.org/10.1016/0378-1119(93)90326-x)
- Cao X, Yin T, Miao Q, Li C, Ju X, Sun Y, Jiang J (2012) Molecular characterization and expression analysis of a gene encoding for farnesyl diphosphate synthase from *Euphorbia pekinensis* Rupr. *Mol Biol Rep* 39(2):1487–1492. <https://doi.org/10.1007/s11033-011-0886-z>
- Chen KK, Chen AL (1935) The alkaloid of chin-shih-hu. *J Biol Chem* 111(3):653–658
- Cheng YJ, Li ZX (2019) Both farnesyl diphosphate synthase genes are involved in the production of alarm pheromone in the green peach aphid *Myzus persicae*. *Arch Insect Biochem Physiol* 100(3):e21530. <https://doi.org/10.1002/arch.21530>
- Ci R, Zhang K, Zhu A, Zang W (2020) Dendrobine attenuates isoniazid- and rifampicin-induced liver injury by inhibiting miR-295-5p. *Hum Exp Toxicol* 39(12):1671–1680. <https://doi.org/10.1177/0960327120937047>
- Closa M, Vranová E, Bortolotti C, Bigler L, Arró M, Ferrer A, Gruissem W (2010) The *Arabidopsis thaliana* FPP synthase isozymes have overlapping and specific functions in isoprenoid biosynthesis, and complete loss of FPP synthase activity causes early developmental arrest. *Plant J* 63(3):512–525. <https://doi.org/10.1111/j.1365-3113.2010.04253.x>
- Corbella A, Gariboldi P, Jommi G, Sisti M (1975) Biosynthesis of the terpenoid dendrobine. Early stages of the pathway. *J Chem Soc Chem Commun* 8288–289. <https://doi.org/10.1039/c39750000288>
- Deng Y, Sun M, Xu S, Zhou J (2016) Enhanced (S)-linalool production by fusion expression of farnesyl diphosphate synthase and linalool synthase in *Saccharomyces cerevisiae*. *J Appl Microbiol* 121(1):187–195. <https://doi.org/10.1111/jam.13105>
- Dhar MK, Koul A, Kaul S (2013) Farnesyl pyrophosphate synthase: a key enzyme in isoprenoid biosynthetic pathway and potential molecular target for drug development. *N Biotechnol* 30(2):114–123. <https://doi.org/10.1016/j.nbt.2012.07.001>

- Dozier JK, Distefano MD (2012) An enzyme-coupled continuous fluorescence assay for farnesyl diphosphate synthases. *Anal Biochem* 421(1):158–163. <https://doi.org/10.1016/j.ab.2011.10.038>
- Feng Y, Jia B, Feng Q, Zhang Y, Chen Y, Meng J (2020) Dendrobine attenuates gestational diabetes mellitus in mice by inhibiting Th17 cells. *Basic Clin Pharmacol Toxicol*. <https://doi.org/10.1111/bcpt.13524>
- Flynn CM, Schmidt-Dannert C (2018) Sesquiterpene synthase-3-hydroxy-3-methylglutaryl coenzyme a synthase fusion protein responsible for hirsutene biosynthesis in *Stereum hirsutum*. *Appl Environ Microbiol* 84(11). <https://doi.org/10.1128/aem.00036-18>
- Frick S, Nagel R, Schmidt A, Bodemann RR, Rahfeld P, Pauls G, Brandt W, Gershenzon J, Boland W, Burse A (2013) Metal ions control product specificity of isoprenyl diphosphate synthases in the insect terpenoid pathway. *Proc Natl Acad Sci USA* 110(11):4194–4199. <https://doi.org/10.1073/pnas.1221489110>
- Gao R, Yu D, Chen L, Wang W, Sun L, Chang Y (2019) Cloning and functional analysis of squalene synthase gene from *Dryopteris fragrans* (L.) Schott. *Protein Expr Purif* 155:95–103. <https://doi.org/10.1016/j.pep.2018.07.011>
- Göbel A, Breining D, Rauner M, Hofbauer LC, Rachner TD (2019) Induction of 3-hydroxy-3-methylglutaryl-CoA reductase mediates statin resistance in breast cancer cells. *Cell Death Dis* 10(2):91. <https://doi.org/10.1038/s41419-019-1322-x>
- Gong DY, Chen XY, Guo SX, Wang BC, Li B (2021) Recent advances and new insights in biosynthesis of dendrobine and sesquiterpenes. *Appl Microbiol Biotechnol* 105(18):6597–6606. <https://doi.org/10.1007/s00253-021-11534-1>
- Han SW, Chae JB, Jo YS, Cho YK, Kang JG, Shin NS, Youn HJ, Youn HY, Nam HM, Kim HJ, Kang HE, Chae JS (2021) First detection of *Borrelia* and *Rickettsia* species from *Ornithodoros* ticks in the Republic of Korea. *Ticks Tick Borne Dis* 12(4):101689. <https://doi.org/10.1016/j.ttbdis.2021.101689>
- Inubushi Y, Sasaki Y, Tsuda Y, Yasui B, Konita T, Matsumoto J, Katarao E, Nakano J (1963) Structure of dendrobine. *Yakugaku Zasshi* 83:1184–1186. https://doi.org/10.1248/yakushi1947.83.12_1184
- Kajiura H, Suzuki N, Tokumoto Y, Yoshizawa T, Takeno S, Fujiyama K, Kaneko Y, Matsumura H, Nakazawa Y (2017) Two *Eucommia* farnesyl diphosphate synthases exhibit distinct enzymatic properties leading to end product preferences. *Biochimie* 139:95–106. <https://doi.org/10.1016/j.biochi.2017.05.001>
- Kaneko KT (1970) Synthetic studies of dendrobine I synthesis of the skeleton of dendrobine. *Tetrahedron Lett*. [https://doi.org/10.1016/S0040-4039\(00\)99728-4](https://doi.org/10.1016/S0040-4039(00)99728-4)
- Keim V, Manzano D, Fernández FJ, Closa M, Andrade P, Caudepón D, Bortolotti C, Vega MC, Arró M, Ferrer A (2012) Characterization of *Arabidopsis* FPS isozymes and FPS gene expression analysis provide insight into the biosynthesis of isoprenoid precursors in seeds. *PLoS ONE* 7(11):e49109. <https://doi.org/10.1371/journal.pone.0049109>
- Kenneth JL, Thomas DS (2002) Analysis of relative gene expression data using real-time quantitative PCR and the 2- $\Delta\Delta$ CT method. *Methods* 25:402–408. <https://doi.org/10.1006/meth.2001.1262>
- Kim HY, Kim DK, Bae SH, Gwak H, Jeon JH, Kim JK, Lee BI, You HJ, Shin DH, Kim YH, Kim SY, Han SS, Shim JK, Lee JH, Kang SG, Jang H (2018) Farnesyl diphosphate synthase is important for the maintenance of *glioblastoma stemness* *Exp Mol Med* 50(10):1–12. <https://doi.org/10.1038/s12276-018-0166-2>
- King HL Jr, Rilling HC (1977) Avian liver prenyltransferase. The role of metal in substrate binding and the orientation of substrates during catalysis. *Biochemistry* 16(17):3815–3819. <https://doi.org/10.1021/bi00636a015>
- Lee JS, Pan JJ, Ramamoorthy G, Poulter CD (2017) Structure-function studies of *Artemisia tridentata* farnesyl diphosphate synthase and chrysanthemyl diphosphate synthase by site-directed mutagenesis and morphogenesis. *J Am Chem Soc* 139(41):14556–14567. <https://doi.org/10.1021/jacs.7b07608>
- Lee Y, Rochette EM, Kim J, Chen DY (2017) An asymmetric pathway to dendrobine by a transition-metal-catalyzed cascade process. *Angew Chem Int Ed Engl* 56(40):12250–12254. <https://doi.org/10.1002/anie.201705713>
- Lee ED, Navas KI, Portnoy DA (2020) The nonmevalonate pathway of isoprenoid biosynthesis supports anaerobic growth of *Listeria monocytogenes*. *Infect Immun* 88(2). <https://doi.org/10.1128/iai.00788-19>
- Li MM, Zhang BX, He SB, Zheng R, Zhang YL, Wang Y (2015) Elucidating hypoglycemic mechanism of *Dendrobium nobile* through auxiliary elucidation system for traditional Chinese medicine mechanism. *China J Chin Materia Med* 40(19):3709–3712. <https://doi.org/10.4268/cjcm.20151903>
- Li Q, Ding G, Li B, Guo SX (2017) Transcriptome analysis of genes involved in dendrobine biosynthesis in *Dendrobium nobile* Lindl. infected with mycorrhizal fungus MF23 (*Mycena sp.*). *Sci Rep* 7(1):316. <https://doi.org/10.1038/s41598-017-00445-9>
- Li ZQ, Zhou HQ, Ouyang Z, Dai J, Han BX (2021) Comparison of active ingredients and protective effects of *Dendrobium huoshanense* of different growth years on acute liver injury. *Zhongguo zhongyao zazhi = China journal of Chinese materia medica* 46(2):298–305. <https://doi.org/10.19540/j.cnki.cjcm.20201023.102>
- Luo AX, He XJ, Zhou SD, Fan YJ, Luo AS, Chun Z (2010) Purification, composition analysis and antioxidant activity of the polysaccharides from *Dendrobium nobile* Lindl. *Carbohydr Polym* 79(4):1014–1019. <https://doi.org/10.1016/j.carbpol.2009.10.033>
- Lv LL, Liu B, Liu J, Li LS, Shi JS (2020) *Dendrobium nobile* linal alkaloids ameliorate cognitive dysfunction in senescence accelerated SAMP8 Mice by decreasing amyloid- β aggregation and enhancing autophagy activity. *J Alzheimer's disease: JAD* 76(2):1–13. <https://doi.org/10.3233/JAD-200308>
- Nie X, Chen Y, Li W, Lu Y (2020) Anti-aging properties of *Dendrobium nobile* Lindl.: from molecular mechanisms to potential treatments. *J Ethnopharmacol* 257:112839. <https://doi.org/10.1016/j.jep.2020.112839>
- Pérez-Castrillón JL, Zarrabeitia MT, Abad L, Vega G, Ruiz-Mambrilla M, González-Sagredo M, Dueñas-Laita A, Riancho JA (2014) Polymorphisms of the farnesyl diphosphate synthase gene modulate bone changes in response to atorvastatin. *Rheumatol Int* 34(8):1073–1077. <https://doi.org/10.1007/s00296-013-2914-x>
- Romanelli MG, Lorenzi P, Sangalli A, Diani E, Mottes M (2009) Characterization and functional analysis of cis-acting elements of the human farnesyl diphosphate synthetase (FDPS) gene 5' flanking region. *Genomics* 93(3):227–234. <https://doi.org/10.1016/j.ygeno.2008.11.002>
- Rubat S, Varas I, Sepúlveda R, Almonacid D, González-Nilo F, Agosin E (2017) Increasing the intracellular isoprenoid pool in *Saccharomyces cerevisiae* by structural fine-tuning of a bifunctional farnesyl diphosphate synthase. *FEMS Yeast Res* 17(4). <https://doi.org/10.1093/femsyr/fox032>
- Sando T, Takeno S, Watanabe N, Okumoto H, Kuzuyama T, Yamashita A, Hattori M, Ogasawara N, Fukusaki E, Kobayashi A (2008) Cloning and characterization of the 2-C-methyl-D-erythritol 4-phosphate (MEP) pathway genes of a natural-rubber producing plant, *Hevea brasiliensis*. *Biosci Biotechnol Biochem* 72(11):2903–2917. <https://doi.org/10.1271/bbb.80387>
- Sha CK, Chiu RT, Yang C (1997) Total synthesis of (–)-dendrobine via α -carbonyl radical cyclization. *J Am Chem Soc* 119(18):4130–4135. <https://doi.org/10.1021/ja964343z>
- Sharifirad A, Mohammadian S, Yakhchali B, Mehrpooyan S, Fatemi SS (2016) Characterization of a farnesyl diphosphate synthase gene from *Penicillium brevicompactum* MUCL 19011. *Biotechnol Lett* 38(1):71–79. <https://doi.org/10.1007/s10529-015-1943-9>
- Song JI, Kang YJ, Yong HY, Kim YC, Moon A (2012) Denbinobin, a phenanthrene from *dendrobium nobile*, inhibits invasion and induces apoptosis in SNU-484 human gastric cancer cells. *Oncol Rep* 27(3):813–818. <https://doi.org/10.3892/or.2011.1551>
- Srivastava PL, Daramwar PP, Krithika R, Pandreka A, Shankar SS, Thulasiram HV (2015) Functional characterization of novel sesquiterpene synthases from Indian sandalwood, *Santalum album*. *Sci Rep* 5:10095. <https://doi.org/10.1038/srep10095>
- Suzuki HK, Ito I (1932) Study on the alkaloids of traditional Chinese medicine *Dendrobium nobile* *J Pharm Soc Japan* 52(12):11
- Vögeli B, Engilberge S, Girard E, Riobé F, Maury O, Erb TJ, Shima S, Wagner T (2018) Archaeal acetoacetyl-CoA thiolase/HMG-CoA synthase complex channels the intermediate via a fused CoA-binding site. *Proc Natl Acad Sci U S A* 115(13):3380–3385. <https://doi.org/10.1073/pnas.1718649115>
- Wang J, Li Y, Liu D (2014) Cloning and characterization of farnesyl diphosphate synthase gene involved in triterpenoids biosynthesis from *Poria cocos* *Int J Mol Sci* 15(12):22188–22202. <https://doi.org/10.3390/ijms151222188>
- Wang P, Chen X, Wang H, Huang S, Cai C, Yuan J, Zhu G, Xu X, Mei W, Dai H (2019) Four New Picrotoxane-Type Sesquiterpenes From *Dendrobium nobile* Lindl. *Front Chem* 7:812. <https://doi.org/10.3389/fchem.2019.00812>
- Wei G, Eberl F, Chen X, Zhang C, Unsicker SB, Köllner TG, Gershenzon J, Chen F (2020) Evolution of isoprenyl diphosphate synthase-like terpene

synthases in fungi. *Sci Rep* 10(1):14944. <https://doi.org/10.1038/s41598-020-71219-z>

Yamazaki M, Matsuo M, Arai K (1966) Biosynthesis of dendrobine. *Chem Pharm Bull (Tokyo)* 14(9):1058–1059. <https://doi.org/10.1248/cpb.14.1058>

Yang J, Zhu J, Shi L, Li Z, Zhang D, Tian Y, Hao Z (2020) The complete mitochondrial genome of *Lunella coronata correensis* Mitochondrial DNA B Resour 5(1):434–435. <https://doi.org/10.1080/23802359.2019.1704183>

Yu H, Liu M, Yin M, Shan T, Peng H, Wang J, Chang X, Peng D, Zha L, Gui S (2021) Transcriptome analysis identifies putative genes involved in triterpenoid biosynthesis in *Platycodon grandiflorus* *Planta* 254(2):34. <https://doi.org/10.1007/s00425-021-03677-2>

Zha L, Liu S, Su P, Yuan Y, Huang L (2016) Cloning, prokaryotic expression and functional analysis of squalene synthase (SQS) in *Magnolia officinalis* *Protein Expr Purif* 120:28–34. <https://doi.org/10.1016/j.pep.2015.12.008>

Publisher's Note

Springer Nature remains neutral with regard to jurisdictional claims in published maps and institutional affiliations.

Submit your manuscript to a SpringerOpen[®] journal and benefit from:

- ▶ Convenient online submission
- ▶ Rigorous peer review
- ▶ Open access: articles freely available online
- ▶ High visibility within the field
- ▶ Retaining the copyright to your article

Submit your next manuscript at ▶ [springeropen.com](https://www.springeropen.com)
